Research Square

Preprints are preliminary reports that have not undergone peer review.
They should not be considered conclusive, used to inform clinical practice,
or referenced by the media as validated information.

MyD88 in Hepatic Stellate Cells Promotes the Development of Alcoholic Fatty Liver via the AKT Pathway

Yukun Li
Beijing Jiaotong University
Miaomiao Wei
Beijing Jiaotong University
Qi Yuan
Beijing Jiaotong University
Yu Liu
Beijing Jiaotong University
Tian Tian
Beijing Jiaotong University
Lingling Hou
Beijing Jiaotong University https://orcid.org/0000-0001-9857-3074
Jinhua Zhang (zhangjh@bjtu.edu.cn)
College of life sciences and bioengineering, Beijing jiaotong university https://orcid.org/0000-0001-8957-8893

Research Article

Keywords: MyD88, hepatic stellate cells, alcoholic fatty liver, Osteopontin

Posted Date: November 3rd, 2021

DOI: https://doi.org/10.21203/rs.3.rs-1030228/v1

License: This work is licensed under a Creative Commons Attribution 4.0 International License.
Read Full License

Abstract

Myeloid differentiation primary response gene 88 (MyD88), an adaptor protein in the TLRs signaling pathway, is expressed in various liver cells including hepatocytes, Kupffer cells and hepatic stellate cells (HSCs). However, the specific role of MyD88 in HSCs in alcoholic fatty liver (AFL) has not been well investigated. Here, to study the role of MyD88 in HSCs in the development of AFL and its related molecular mechanism, chronic-binge ethanol mice models were established in mice with specific MyD88 knockout in quiescent ($MyD88^{GFAP-KO}$) and activated HSCs ($MyD88^{SMA-KO}$), respectively. The results showed that the expression of MyD88 in HSCs was significantly increased in ethanol-induced liver tissues of wild-type mice. MyD88 deficiency in quiescent HSCs inhibited inflammation and lipogenesis, but in activated HSCs it only inhibited inflammation under the ethanol feeding condition. Further mechanism studies found that MyD88 promoted the osteopontin (OPN) secretion of HSCs, which further activated the AKT signaling pathway of hepatocytes and upregulated lipogenic gene expression to promote fat accumulation. In addition, OPN also promotes inflammation by activating p-STAT1. Thus, MyD88 may represent a potential candidate target for the prevention and targeted therapy in AFL, and MyD88 inhibitor can be also applied in inhibiting adipogenesis.

Key Message

- The expression of MyD88 in HSCs was significantly increased in ethanol-induced liver tissues of wild-type mice.
- MyD88 deficiency in quiescent HSCs inhibited inflammation and lipogenesis under the ethanol feeding condition.
- MyD88 deficiency in activated HSCs only inhibited inflammation under the ethanol feeding condition.
- MyD88 promoted the OPN secretion of HSCs, which further activated the AKT signaling pathway of hepatocytes and upregulated lipogenic gene expression to promote fat accumulation.
- OPN also promotes inflammation by activating p-STAT1.

1. Introduction

Excessive alcohol consumption is a leading cause of alcoholic liver disease (ALD), which is characterized by a spectrum of liver pathology ranging from fatty liver, alcoholic hepatitis, fibrosis, cirrhosis and hepatocellular carcinoma (HCC)[1, 2]. Alcoholic fatty liver (AFL) is the initial stage of the disease, and increasing evidences suggest that it has potentially pathologic condition[3, 4]. To date, several molecular mechanisms regulating hepatic lipid metabolism have been elucidated[5, 6]. Ethanol metabolism–associated oxidative stress and chemokines have been reported to play critical roles in the development of AFL[7, 8]. Although potential therapeutic methods for AFL have been developed for decades, effective therapies for AFL are still in great needs.

AFL is a kind of disorder in lipid metabolism, which is mainly manifested by hepatic steatosis. Steatosis is defined as intrahepatic fat of at least 5% of liver weight, which is characterized by the increase of triglyceride and cholesterol esters and is the first manifestation of chronic ethanol-induced fatty liver[9]. Enhanced lipid synthesis results from a higher expression of lipogenic enzymes and cytokines, such as fatty acid synthase (FAS), acyl CoA carboxylase (ACC), ATP citrate lyase (ACL) and malic enzyme (ME), which are regulated by sterol regulatory element binding protein-1c (SREBP-1c)[10, 11]. Hepatic ethanol oxidation triggers the translocation of SREBP-1c. SREBP-1c is matured by proteolysis and becomes a SREBP protein fragment with transcriptional activity, which enters the nucleus and enhances lipogenic gene expression. Regulation of lipid metabolism can be used as a target for prevention or treatment of fatty liver related steatosis.

Hepatic stellate cells (HSCs) are a kind of non-parenchymal cells in the liver. In a healthy liver, HSCs are in a quiescent state and contain a large number of lipid droplets storing vitamin A[12]. When the liver is damaged, HSCs are activated into myofibroblasts, express α-smooth actin(α-SMA), and secrete a large number of extracellular matrix proteins[13]. HSCs play a role in AFL, hepatitis, liver fibrosis, liver cirrhosis and liver cancer. Activated HSCs can promote liver fibrosis and regeneration of liver epithelial cells. In addition, activated HSCs release a variety of growth factors and promote tumor growth[14]. Activated HSCs can also recruit macrophages and promote the secretion of TNF-α, which binds to the corresponding receptors on hepatocytes to induce the expression of fat related genes. It has also been reported that alcohol stimulates HSCs to produce more 2-arachidonoylglycerol (2-AG), which can increase the expression of fat related genes in hepatocytes through paracrine pathway and promote the occurrence of AFL[15]. At present, the mechanism of HSCs regulating lipogenesis is not very clear.

Toll-like receptors (TLRs) recognize pathogen-associated molecular patterns (PAMPs) and damage-associated molecular patterns (DAMPs) in the form of dimers and further activate innate immune system[16, 17]. TLRs are expressed in many different cell types of liver with different expression patterns and play important roles in chronic liver diseases through the interaction between different cell types. Myeloid differentiation primary response gene 88 (MyD88) is a key adaptor molecule for the most TLRs (except TLR3) and IL-1 receptor families and is mainly responsible for transmitting signals to the downstream, activating NF-κB and MAPK family members and leading to the production of pro-inflammatory or anti-inflammatory cytokines and type I interferon[18]. MyD88 plays significant roles in inflammation related diseases. In addition, it is also involved in regulating the metabolism of energy, glucose and lipids in a variety of cells[19]. The physiological functions of MyD88 varied in different tissues and cell types.

Neuronal MyD88 dependent signal was a key regulator of diet induced insulin resistance in vivo. It has been reported that MyD88 specific deletion in the central nervous system could prevent peripheral glucose metabolism impairment induced by HFD, palmitate and blunted insulin resistance[20]. However, systemic knockout of MyD88 exacerbate the impaired glucose tolerance induced by high-fat diet[21] and increase the risk of diabetes in mice[22]. Hepatocyte specific deletion of MyD88 contributes to glucose intolerance, inflammation and liver insulin resistance independently of body weight and adiposity, which

has been proved in the album-MyD88 KO mice with high-fat diet model and are partly due to differences in gene expression and transcription factor activity[23]. Furthermore, MyD88 in endothelial cells and myeloid cells also induces inflammation and insulin resistance in high-fat diet[24]. Nagy LE et al. found that deficiency of MyD88 in myeloid cells inhibited the occurrence of steatosis and inflammation in myeloid-specific MyD88-deficient ($MyD88^{LysM-KO}$) mice with Lieber-DeCarli ethanol containing diet model[25]. MyD88 in macrophages(Kupffer cells)promotes ethanol-induced liver injury and steatosis in the high-fat diet model[26]. However, the role of MyD88 in HSCs in the development of AFL and its mechanism remains unclear.

For this purpose, mice with genetic deletion of MyD88 in quiescent HSCs ($MyD88^{GFAP-KO}$) and activated HSCs ($MyD88^{SMA-KO}$) matched with littermate controls were used in a chronic-binge ethanol model for studying the HSC-specific role of TLR signaling and its related molecular mechanism in ALD. We found that MyD88 was mainly expressed in HSCs and alcohol-induced liver injury and inflammation in mice. MyD88 in quiescent HSCs also promotes hepatic fat accumulation. Further mechanistic studies found that MyD88 in HSCs promotes liver fat accumulation mainly by secreting OPN, activating the AKT pathway and upregulating lipogenic gene expression. Taken together, these results indicated that MyD88 may represent a potential candidate for the prevention and treatment of AFL.

2. Materials And Methods

2.1 Mice

$MyD88^{flox/flox}$ ($MyD88^{fl/fl}$), GFAP-Cre[27] and SMA-Cre mice[27-30] on a C57BL/6 background have been previously described. Mice with a conditional knockout of MyD88 in GFAP-expressing quiescent HSCs ($MyD88^{GFAP-KO}$) were generated by crossing $MyD88^{fl/fl}$ and GFAP-Cre mice. And mice with a conditional knockout of MyD88 in SMA-expressing activated HSCs ($MyD88^{SMA-KO}$) were generated by crossing $MyD88^{fl/fl}$ and SMA-Cre mice. Eight-week-old male mice were used. All mice were bred in specific pathogen-free and humidity- and temperature-controlled microisolator cages with a 12-hour light/dark cycle at the Institute of Biophysics Chinese Academy of Sciences. All animal studies were performed after being approved by the Institutional Laboratory Animal Care and Use Committee of the Institute of Biophysics, Chinese Academy of Sciences.

2.2 Chronic-binge ethanol mice models

Chronic-binge ethanol mice models was established as described previously[31]. Ten week old male C57BL/6 mice, $MyD88^{GFAP-KO}$and $MyD88^{SMA-KO}$ mice were fed with liquid control diet (TROPHIC, Nantong, China) for 2 days to adapt liquid diet at 4pm every afternoon and then were divided into two groups randomly and five mice in each group: ethanol group was fed with liquid Lieber-DeCarli diet (TROPHID, Nantong, China) containing 1% ethanol for 2 days, increasing to 2% ethanol for 2 days, and 4% ethanol for 7 days and finally maintained at 5% ethanol for 10 days at 4pm every afternoon, followed by a single dose gavage of 31.5% ethanol (5 g/kg body weight) on the last day. Control mice were fed

with pair-fed diet and finally given a single dose gavage of isocaloric dextrin maltose. Mice were always given a gavage in the morning and euthanized 9 h after receiving a gavage. For the ethanol feeding period, food intake of the ethanol-fed mice was recorded, and the weight-matched control feeding mice were pair-fed with the same volume of the control diet, so that ethanol- and pair-fed mice consumed equal amounts of diet and ingested the same energy. Besides the body weight of mice was recorded every day.

2.3 Cell culture

The LX-2 and HepG2 cell lines were obtained from the American Type Culture Collection (ATCC; Manassas, VA, USA). These cells were cultured in DMEM (BI, Israel) supplemented with 10% fetal bovine serum (FBS, BI) and 1% penicillin/streptomycin at 37°C with 5% CO_2. In the experimental groups, LX-2 cells were exposed to ST2825 (10 μM) (MedChemExpress, USA) for 2 h, and then were challenged with TLR1/2 agonist (Pam3CSK4, 100 ng/mL), TLR4 agonist (LPS, 1 mg/mL) and palmitic acid (400 μM) (Sigma, USA) respectively for 24 h. In the control groups, LX-2 cells were directly challenged with TLR1/2 agonist (Pam3CSK4, 100 ng/mL), TLR4 agonist (LPS, 1 mg/mL) and palmitic acid (400 μM) (Sigma, USA) respectively for 24 h. To induce excessive lipid accumulation, HepG2 cells were cultured in DMEM medium with 20 μM AKT inhibitor (CSNpharm, USA) for 24h, then 400 μM palmitic acid and 200 ng/mL recombinant protein OPN (Cloud-Clone Corp, China) for 24h[32].

2.4 Isolation of HSCs

Isolation of primary hepatic stellate cells was performed as previously described[30]. 10-week-old mice were used to isolate primary hepatic stellate cells. Briefly, primary HSCs were isolated from livers by in situ perfusion and density gradient centrifugation. The mice were anesthetized with 3% ethyl carbamate and treated with phosphate belanced solution and sterile collagenase for liver perfusion. And the liver was removed, cut it into small pieces, and was placed in the digestive juice at 37°C for 30 minutes. Filtered cells were centrifuged at 50×*g* for 2 min to remove hepatocytes. The remaining non-parenchymal cell (NPC) fraction was collected, washed, and isolated by a 10% and 40% Optiprep (Axis-Shield, Scotland) gradient system, respectively[33]. The purity of the HSC fraction was estimated based on the autofluorescence signal. Cell viability was examined by Trypan blue exclusion. Both the cell purity and viability were greater than 90%.

2.5 Biochemical assays of blood and liver tissues

Blood samples of mice were collected by the eyeball and centrifuged at 3000·*g* for 10 minutes to obtain serum. Serum alanine aminotransferase (ALT), aspartate aminotransferase (AST), cholesterol (Cho) and triglyceride (TG) levels were detected by Pony Testing International Group (Beijing, China). Liver tissues were homogenized in cold phosphate-buffered saline (PBS) and centrifuged at 2400 *g* for 10 minutes to obtain supernatant, and TG and Cho levels in supernatant were measured by Pony Testing International Group (Beijing, China).

2.6 Histology and immunostaining

Paraffin or cryostat sections of liver tissue were prepared as described previously[34]. The sliced liver paraffin sections were stained with hematoxylin and eosin (H&E) (Zhongshanjinqiao, Beijing, China) and Sirius Red, respectively. To detect hepatic fat accumulation, cryostat liver sections were stained with Oil Red O. For immunofluorescence detection, the cryostat sections were respectively incubated with anti-F4/80, anti-Gr-1, anti-CD11b (1:200; BD Pharmingen, San Diego, CA), anti-MyD88 and anti-GFAP antibodies (1:200; Abcam, Cambridge, UK), and followed by incubation with Alexa Fluor 488- or 594-conjugated secondary antibodies (1:500; Invitrogen, Carlsbad, CA, USA). Eventually, cell nuclei were stained with DAPI. Results were evaluated under the microscope (DP71, OLYMPUS) of both bright-field and fluorescence microscopy.

2.7 Quantitative real-time polymerase chain reaction (qRT-PCR)

Total RNA was isolated from frozen liver tissues and cells respectively by TRIzol reagent (Invitrogen, USA), and then up to 0.5μg of RNA was reverse transcribed by Prime Script RT Master Mix Kit (MedChemExpress, Princeton, NJ, USA). cDNA was duplicated by SYBR Premix ExTaqTM Kit (MedChemExpress, Princeton, NJ, USA). The primer sequences are listed in Supplementary Table 1. Data were analyzed using the $2^{-\Delta\Delta Ct}$ method and normalized to GAPDH expression[35].

2.8 Western blot analysis

Western blot was performed as previously described[36]. Tissue and cell extracts were analyzed with the following primary antibodies: anti-MyD88 (Abcam, Cambridge, UK), anti-AKT, anti-p-AKT, anti-STAT1 and anti-p-STAT1 antibodies (Cell Signaling Technology, USA). HRP-conjugated goat anti-mouse IgG and goat anti-rabbit IgG were used as secondary antibodies. Blots were scanned using a Clinx Science Instrument. All specific bands were quantified with the ImageJ automated Digitizing System.

2.9 Quantitative and statistical analysis

All the data were expressed as means±SEM and analyzed using GraphPad Prism software. Differences between the two groups were compared using two-tailed unpaired Student's t-test analysis. One-way ANOVA tests with a Bonferroni correction were used for multiple comparisons. For all tests, $p < 0.05$ was considered statistically significant. $p < 0.01$ was considered extremely significant.

3. Results

3.1 Expression of MyD88 in HSCs is upregulated in the liver of AFL mice

To explore the relationship between the expression of MyD88 in mouse liver and the development of AFL, C57BL/6 mice were administered ethanol to generate a chronic-binge ethanol mice models, which is widely used for the pathogenetic study of AFL. Liver tissues were harvested after AFL was established (Fig. 1a). As shown in Fig. 1b, c, the protein expression level of MyD88 was significantly upregulated in

the livers of ethanol-fed mice compared with control mice detected by Western blot. MyD88^{+} cells in the liver tissues were further detected by immunofluorescence staining. Consistently, ethanol feeding led to a significant increase of the number of MyD88^{+} cells. Double immunofluorescence staining revealed that most of HSCs (GFAP^{+} cells) of AFL mice expressed MyD88 (Fig. 1d). The results clearly demonstrated that MyD88 expression in HSCs of WT mice was upregulated under the ethanol feeding condition.

3.2 MyD88 deficiency in HSCs attenuates ethanol-induced liver injury

To investigate the contribution of MyD88 in HSCs in liver injury, MyD88 $^{GFAP-KO}$ and MyD88 $^{SMA-KO}$ mice were generated by Cre loxp system, and control littermates were used in a chronic-binge ethanol model (Supplementary Fig. 1). There is no significant difference of the body weight between MyD88 $^{GFAP-KO}$ and MyD88$^{fl/fl}$ mice, MyD88 $^{SMA-KO}$ and MyD88$^{fl/fl}$ mice under the ethanol feeding condition (Fig. 2a, b). To characterize the pathology associated with ethanol feeding in MyD88$^{GFAP-KO}$, MyD88^{SMA-KO} and MyD88$^{fl/fl}$ mice, the liver tissues from each group were collected for further evaluation. The liver/body weights of the MyD88$^{GFAP-KO}$ mice were significantly increased compared with those of MyD88$^{fl/fl}$ mice (Fig. 2c). However, there was no significant differences of the liver/body weights between MyD88^{SMA-KO} mice and MyD88$^{fl/fl}$ mice (Fig. 2d). We further examined the serum ALT and AST levels in MyD88$^{fl/fl}$, MyD88$^{GFAP-KO}$ and MyD88^{SMA-KO} mice under the ethanol feeding condition. The results showed that the ALT level was significantly decreased in MyD88$^{GFAP-KO}$ mice compared with that in MyD88$^{fl/fl}$ mice (Fig. 2e, f) and the AST level was significantly decreased in MyD88^{SMA-KO} mice compared with that in control mice (Fig. 2g, h). Further H&E staining showed that both MyD88$^{GFAP-KO}$ and MyD88^{SMA-KO} mice had reduced inflammatory cell infiltration, hepatocyte cell death and steatosis compared with MyD88$^{fl/fl}$ mice (Fig. 2i, j). These results indicated that MyD88 knockout in HSCs significantly reduced liver injury.

3.3 MyD88 deficiency in HSCs attenuates ethanol-induced liver inflammation

To investigate the effect of MyD88 in HSCs on inflammation, the infiltration of immune cells was detected by immunofluorescence staining. The results showed that the infiltration of F4/80^{+} macrophages, Gr1^{+} neutrophil and CD11b^{+} monocyte was significantly reduced in MyD88$^{GFAP-KO}$ mice and MyD88^{SMA-KO} compared with MyD88$^{fl/fl}$ mice under the ethanol feeding condition (Fig. 3a-d). We further examined the gene expression of a series of pro-inflammatory cytokines in MyD88$^{fl/fl}$, MyD88$^{GFAP-KO}$ and MyD88^{SMA-KO} mice under the ethanol feeding condition. As shown in Fig. 3e, f, mRNA levels of the proinflammatory cytokines interleukin-6 (IL-6), IL-1β, tumor necrosis factor α (TNF-α) and monocyte chemoattractant protein-1 (MCP-1) were significantly down-regulated in livers of MyD88$^{GFAP-KO}$ and MyD88^{SMA-KO} mice compared with that of MyD88$^{fl/fl}$ mice after ethanol feeding. In summary, MyD88 knockout in HSCs can significantly attenuates hepatic inflammation.

3.4 MyD88 deficiency in HSCs attenuates fat accumulation

AFL is mainly caused by continuous alcohol intake. The fat in the liver becomes small lipid droplets in the early stage of steatosis, and subsequently expands into large lipid droplets. Fat accumulation in the liver is often accompanied by elevated Cho and TG. The levels of Cho and TG in mouse serum and liver tissue were further detected by biochemical indicators.

The results showed that except serum TG, the levels of serum Cho,hepatic Cho and hepatic TG were significantly decreased in the $MyD88^{GFAP-KO}$ mice compared with those in $MyD88^{fl/fl}$ mice (Fig. 4a, b). However, there was no significantly difference in serum and hepatic TG and Cho between $MyD88^{SMA-KO}$ and $MyD88^{fl/fl}$ mice (Fig. 4c, d).

In order to further verify the production of TG and other neutral fats in the liver tissues, the liver tissues of $MyD88^{GFAP-KO}$, $MyD88^{SMA-KO}$ and $MyD88^{fl/fl}$ mice were stained with Oil Red O. As shown in Fig. 4e, the accumulation of lipid droplet in the liver tissues of $MyD88^{GFAP-KO}$ mice was significantly reduced compared with $MyD88^{fl/fl}$ mice. The accumulation of lipids occurred in hepatocytes. Consistently, the mRNA levels of lipogenesis genes such as SREBP1, SCD1, ACC1 and FANS were significantly downregulated in the liver tissues of $MyD88^{GFAP-KO}$ mice compared with $MyD88^{fl/fl}$ mice (Fig. 4f). However, there was no significant differences in hepatic fat accumulation and related lipogenesis genes between $MyD88^{SMA-KO}$ and control mice (Fig. 4g, h). In addition, results from Sirius Red staining demonstrated that no obvious fibrosis occurred, and MyD88 deficiency in quiescent HSCs has no obvious effects on liver fibrosis in this model (Supplementary Fig. 2). These results indicated that MyD88 deficiency in HSCs significantly inhibited hepatic fat accumulation.

3.5 MyD88 deficiency in quiescent HSCs inhibits the expression of OPN

To study how the MyD88 in quiescent HSCs affected the ethanol-induced inflammatory and adipogenesis in liver cells, the GEO database (GSE151158) was used to analyze the gene expression levels in the livers of 21 healthy people and 40 fatty liver patients and found that the expression level of OPN gene in the livers of fatty liver patients was significantly increased (Fig. 5a). Related evidence also showed that OPN could promote adipogenesis[37]. Then the expression of OPN in the livers of $MyD88^{GFAP-KO}$ and $MyD88^{fl/fl}$ mice was detected by RT-qPCR. As shown in Fig. 5b, the expression level of OPN in the liver of $MyD88^{GFAP-KO}$ mice was significantly decreased compared with $MyD88^{fl/fl}$ mice, and there is no obvious change in $MyD88^{GFAP-KO}$ mice (Fig. 5c). Immunohistochemical staining further confirmed that the OPN protein expression in the liver of $MyD88^{GFAP-KO}$ mice was also significantly reduced (Fig. 5d).

To explore whether MyD88 deficiency in quiescent HSCs would affect the secretion of OPN, the HSCs line LX-2 was treated with MyD88 inhibitor ST2825 for 2h and then with TLR1/2 and TLR4 agonists for 24h. The results showed that the agonist treatment promoted the expression of OPN in LX-2 cells, and the *OPN* expression was significantly reduced after adding the MyD88 inhibitor ST2825, and the TLR4 agonist had the most significant effects (Fig. 5e). The above results showed that the TLR4 signaling pathway played a key role in regulating the expression of OPN. After activation of the TLR4 signaling pathway by palmitic

acid, the expression of MyD88 and OPN genes were detected by RT-qPCR. The result indicated that ST2825 significantly inhibited the expression of MyD88 (Fig. 5f), and palmitic acid significantly promoted the expression of OPN, while ST2825 inhibitor significantly reduced the OPN expression (Fig. 5g). The results showed that the expression of OPN in HSCs was regulated by MyD88.

To further study the effect of OPN secreted by HSCs on the adipogenesis of HepG2 cells, HepG2 cells were treated with palmitic acid to induce fatty liver-like cells, and the expression of hepatic lipogenesis genes in HepG2 cells was detected by RT-qPCR. The mRNA levels of SREBP1, SCD1, ACC1 and FANS in HepG2 cells were significantly up-regulated after palmitic acid treatment (Fig. 5h). Subsequently, the recombinant protein OPN was added exogenously to explore its effect on the adipogenesis of HepG2 cells. RT-qPCR results showed that OPN significantly promoted the expression of adipogenesis-related genes SCD1、FANS、SREBP and ACC1 in HepG2 cells (Fig. 5h). The results indicated that OPN secreted by HSCs significantly promoted adipogenesis in HepG2 cells.

3.6 MyD88 promoted liver fat accumulation and inflammation via the AKT pathway and STAT1 pathway respectively

To elucidate the underlying mechanism responsible for ethanol-induced hepatic lipid accumulation, we tested the signaling pathways in which MyD88 may be involved during liver fat accumulation and inflammation. The results showed that there were no significant differences in the total protein level of AKT in the liver tissues between $MyD88^{GFAP-KO}$ mice and $MyD88^{fl/fl}$ mice (Fig. 6a), but the p-AKT expression was significantly increased in the liver of $MyD88^{GFAP-KO}$ mice compared with $MyD88^{fl/fl}$ mice (Fig. 6a, b). Meanwhile, it was found that there were no significant differences in the total protein level of STAT1 in the liver of $MyD88^{GFAP-KO}$ mice and $MyD88^{fl/fl}$ mice, but the phosphorylation level of STAT1 in $MyD88^{GFAP-KO}$ mice was significantly lower than that of $MyD88^{fl/fl}$ mice (Fig. 6a, b). The AKT and STAT1 signaling pathway was further analyzed in the human hepatoma cell line HepG2. HepG2 cells were pretreated with palmitic acid for 24 hours, and then OPN was added for 24h. The related protein expressions of AKT and STAT1 signaling pathway were detected by Western blot. The results showed that Akt phosphorylation level was significantly decreased and STAT1 phosphorylation level was significantly increased in OPN treatment group compared with the control group (Fig. 6c, d). To further explored whether OPN affected fat accumulation by regulating the phosphorylation of AKT, we added the AKT inhibitor MK-2206 to HepG2 cells to detect the expression of genes related to fat production. RT-qPCR results showed that the expression levels of adipogenesis-related genes SCD1、FANS、SREBP1 and ACC1 were significantly increased after AKT inhibitor treatment (Fig. 6e). The above results suggested that MyD88 enhanced liver fat accumulation via activating AKT pathway and promoted inflammation through STAT1 pathway.

4. Discussion

MyD88 is a key player in ALD. However, due to its wide expression, the cell-type specific contribution of MyD88-mediated signaling to ALD is still unclear. In this study, the specific role of MyD88 in HSCs in AFL has been investigated. We found that deficiency of MyD88 in quiescent HSCs significantly reduced liver injury, inflammation and steatosis, while MyD88 deficiency in activated HSCs (myofibroblasts) could only inhibit the progression of liver injury and inflammation, and had no obvious effects on steatosis. Furthermore, mechanistic studies showed MyD88 regulated OPN secretion of HSCs to active AKT signaling pathways of hepatocytes and upregulate lipogenic gene expression to promote fatty accumulation (Fig. 7). Thus, MyD88 may represent a potential candidate target for the prevention and targeted therapy in AFL.

More evidences showed that TLRs mediated innate immune response was related to liver injury, inflammation, liver fibrosis and liver fat metabolism, which may be attributed to the expression of TLRs in a variety of liver cells, including liver parenchymal cells, Kupffer cells, sinusoidal endothelial cells, HSCs, bile duct epithelial cells and liver dendritic cells[38-40]. TLRs other than TLR3 can bind to corresponding ligands and transmit signals through adapter molecule MyD88, and further activate NF-κB and JNK signal pathway[18]. In this study, we also confirmed the relevance between TLR and liver lipogenesis. We found that MyD88 deficiency in HSCs attenuated ethanol-induced liver inflammation and fat accumulation, and MyD88/TLR4 signaling pathway played a key role in regulating the expression of OPN and is related to the formation of AFL. Nagy LE et al. reported that specific MyD88 deletion in myeloid cells reduced ethanol-induced increases of plasma ALT and hepatic steatosis. Ethanol-induced inflammation and the expression of pro-inflammatory mediators were also attenuated in the livers of $MyD88^{LysM-KO}$ mice[25]. However, Cani PD et al. found that MyD88 deletion in hepatocyte induced profound changes in glucose and lipid metabolism, which specifically showed that liver glycogen and the phosphorylation of insulin-induced AKT decreased, liver lipid and the inflammation of visceral adipose tissue increased[41]. These studies indicate that MyD88 in hepatocytes, myeloid cells, and HSCs may have different effects and mechanism on hepatic steatosis and inflammation.

OPN is a highly phosphorylated glycoprotein and expressed in various cells and widely exists in extracellular matrix, which has important functions on cardiovascular disease, cancer, diabetes, cell viability and wound healing[42], and is also related to the immunity regulation, metabolism and inflammation process[41]. In present study, we found that OPN derived from HSCs acted on hepatocyte, promoted lipogenesis and inflammatory response by inhibiting the phosphorylation of AKT and increasing the phosphorylation of STAT1 respectively. In the meantime, the relevance between OPN and hepatic lipogenesis was also verified in clinical cases. In this study, the gene expression levels of 21 healthy people and 40 patients with fatty liver were analyzed by GEO database (gse151158). It was found that the expression level of OPN was significantly increased in the liver of patients with fatty liver. Consisted with our results, Smid V. et al. reported that OPN was able to promote lipogenesis and could be used as a potential marker of fatty liver[43]. Haber PS et al. also confirmed that OPN is overexpressed in the liver of patients with AFL, especially when HSCs are activated, the expression level of OPN will increase significantly[44]. In addition, MORALES-IBANEZ et al. found that OPN deficiency inhibited liver

damage by constructing OPN-knockout mice and chronic-binge ethanol model[41]. Gómez-Ambrosi J et al. found that OPN deficiency prevented hepatic steatosis via reduction in the expression of molecules involved in the onset of fat accumulation such as Pparg, Srebf1, Fasn, Mogat1, Dgat2 and Cidec in OPN-knockout mice with by a high-fat diet (HFD)[45]. Furthermore, related evidence also reported that OPN participated in the AKT and STAT1 signaling pathways and played a role in steatosis and inflammation. However, GE et al. confirmed that OPN combined with lipopolysaccharide (LPS) reduced the activation of macrophages and the expression of TNF-α, and reduced liver damage and steatosis[46]. The mechanism of OPN on liver injury and steatosis still needs to be further explored. AFL has become a severe issue that threatened human health all over the world[47]. At present, abstinence, nutritional support and glucocorticoid therapy are still the main methods for the treatment of AFL which have respective limitations, effective targeted therapy are in needs. It is essential to deeply understand the mechanism of AFL and provide theoretical and experimental basis for the treatment of AFL[48]. In recent years, it had been found that both innate and adaptive immunity were involved in the development of AFL. TLRs, as a type of pattern recognition receptors, were expressed in various cells in the liver and played a key role in the activation of the immune system[49]. As an important adaptor protein in the TLRs signaling pathway, MyD88 not only regulated the immune response, but also affected the metabolic process. Various cell types are involved in the occurrence of AFL, such as hepatocytes, immune cells and HSCs. Among them, Kupffer cells was the most widely studied, which caused inflammation, liver damage and fatty liver by secreting a large number of inflammatory cytokines such as TNF-α, IL-1 and IL-17[50]. In addition, it had also been found that HSCs not only played a role in the development of liver fibrosis by secreting extracellular matrix, but also promoted lipogenesis by secreting factors such as endocannabinoids. Depending on these results, we further explored the role of MyD88 in HSCs in the development of AFL and its mechanism.

In conclusion, our results demonstrated a mechanism for the pathogenesis of AFL in which MyD88 promoted lipid accumulation and inflammation via the AKT and STAT1 pathway. The present study showed that MyD88 deficiency in quiescent HSCs significantly inhibited ethanol-induced hepatic lipid accumulation, liver injury and inflammation by inhibiting the secretion of OPN. MyD88 could be a target for AFL therapy. Further studies should evaluate if OPN protein treatment can inhibit the progression of AFL.

Declarations

Funding: This work was supported by the National Natural Science Foundation of China (81972689 and 81772497).

Institutional Review Board Statement: All animal studies were performed after being approved by the Institutional Laboratory Animal Care and Use Committee of the Institute of Biophysics, Chinese Academy of Sciences.

Author Contributions:

Jinhua Zhang, Lingling Hou conceived and designed the study; Yukun Li carried out the experiments; Yukun Li and Lingling Hou wrote the manuscript; Yukun Li and Lingling Hou and Miaomiao Wei drafted the manuscript; Yukun Li, Miaomiao Wei, Qi Yuan, Yu Liu, Tian Tian, Lingling Hou and Jinhua Zhang read and approved the final manuscript. All authors have read and agreed to the published version of the manuscript.

Informed Consent Statement: Not applicable.

Data Availability Statement: All relevant data are presented in this paper.

Declaration of Interests: The authors declare no conflict of interest.

References

1. Kong LZ, Chandimali N, Han YH, Lee DH, Kim JS, Kim SU, et al. (2019) Pathogenesis, Early Diagnosis, and Therapeutic Management of Alcoholic Liver Disease. Int J Mol Sci 20(11):2712.
2. Mathurin P, Bataller R (2015) Trends in the management and burden of alcoholic liver disease. J Hepatol 62(1 Suppl):S38-46.
3. Louvet A, Mathurin P (2015) Alcoholic liver disease: mechanisms of injury and targeted treatment. Nat Rev Gastroenterol Hepatol 12(4):231-42.
4. Natalia A Osna TMDJ, Kusum K Kharbanda (2017) Alcoholic Liver Disease: Pathogenesis and Current Management. Alcohol Res 38(2):147-61.
5. Gao B, Bataller R (2011) Alcoholic liver disease: pathogenesis and new therapeutic targets. Gastroenterology 141(5):1572-85.
6. Nagy LE, Ding WX, Cresci G, Saikia P, Shah VH (2016) Linking Pathogenic Mechanisms of Alcoholic Liver Disease With Clinical Phenotypes. Gastroenterology 150(8):1756-68.
7. Chang B, Xu MJ, Zhou Z, Cai Y, Li M, Wang W, et al. (2015) Short- or long-term high-fat diet feeding plus acute ethanol binge synergistically induce acute liver injury in mice: an important role for CXCL1. Hepatology 62(4):1070-85.
8. You M, Jogasuria A, Lee K, Wu J, Zhang Y, Lee YK, et al. (2017) Signal Transduction Mechanisms of Alcoholic Fatty Liver Disease: Emer ging Role of Lipin-1. Curr Mol Pharmacol 10(3):226-36.
9. Gu J, Zhang Y, Xu D, Zhao Z, Zhang Y, Pan Y, et al. (2015) Ethanol-induced hepatic steatosis is modulated by glycogen level in the liver. J Lipid Res 56(7):1329-39.
10. Choi YJ, Shin HS, Choi HS, Park JW, Jo I, Oh ES, et al. (2014) Uric acid induces fat accumulation via generation of endoplasmic reticulum stress and SREBP-1c activation in hepatocytes. Lab Invest 94(10):1114-25.
11. Greuter T, Malhi H, Gores GJ, Shah VH (2017) Therapeutic opportunities for alcoholic steatohepatitis and nonalcoholic steatohepatitis: exploiting similarities and differences in pathogenesis. JCI Insight 2(17):e95354.

12. de Oliveira da Silva B, Ramos LF, Moraes KCM (2017) Molecular interplays in hepatic stellate cells: apoptosis, senescence, and phenotype reversion as cellular connections that modulate liver fibrosis. Cell Biol Int 41(9):946-59.
13. Shang L, Hosseini M, Liu X, Kisseleva T, Brenner DA (2018) Human hepatic stellate cell isolation and characterization. J Gastroenterol 53(1):6-17.
14. Yin C, Evason KJ, Asahina K, Stainier DY (2013) Hepatic stellate cells in liver development, regeneration, and cancer. J Clin Invest 123(5):1902-10.
15. Choi WM, Kim HH, Kim MH, Cinar R, Yi HS, Eun HS, et al. (2019) Glutamate Signaling in Hepatic Stellate Cells Drives Alcoholic Steatosis. Cell Metab 30(5):877-89 e7.
16. Bob J Ignacio TJA, Aaron P Esser-Kahn, Martijn Verdoes (2018) Toll-like Receptor Agonist Conjugation: A Chemical Perspective. Bioconjug Chem 29(3):587-603.
17. Tamtaji OR, Mobini M, Reiter RJ, Azami A, Gholami MS, Asemi Z (2019) Melatonin, a toll-like receptor inhibitor: Current status and future perspectives. J Cell Physiol 234(6):7788-95.
18. Deguine J, Barton GM (2014) MyD88: a central player in innate immune signaling. F1000Prime Rep 6:97.
19. Duparc T, Plovier H, Marrachelli VG, Van Hul M, Essaghir A, Stahlman M, et al. (2017) Hepatocyte MyD88 affects bile acids, gut microbiota and metabolome contributing to regulate glucose and lipid metabolism. Gut 66(4):620-32.
20. Kleinridders A, Schenten D, Konner AC, Belgardt BF, Mauer J, Okamura T, et al. (2009) MyD88 signaling in the CNS is required for development of fatty acid-induced leptin resistance and diet-induced obesity. Cell Metab 10(4):249-59.
21. Charlotte Lefort MVH, Nathalie M Delzenne, Amandine Everard, Patrice D Cani (2019) Hepatic MyD88 regulates liver inflammation by altering synthesis of oxysterols. Am J Physiol Endocrinol Metab 317(1):E99-E108.
22. Bollyky PL, Bice JB, Sweet IR, Falk BA, Gebe JA, Clark AE, et al. (2009) The toll-like receptor signaling molecule Myd88 contributes to pancreatic beta-cell homeostasis in response to injury. PLoS One 4(4):e5063.
23. Wen L, Ley RE, Volchkov PY, Stranges PB, Avanesyan L, Stonebraker AC, et al. (2008) Innate immunity and intestinal microbiota in the development of Type 1 diabetes. Nature 455(7216):1109-13.
24. Everard A, Geurts L, Caesar R, Van Hul M, Matamoros S, Duparc T, et al. (2014) Intestinal epithelial MyD88 is a sensor switching host metabolism towards obesity according to nutritional status. Nat Commun 5:5648.
25. Zhou H, Yu M, Roychowdhury S, Sanz-Garcia C, Pollard KA, McMullen MR, et al. (2017) Myeloid-MyD88 Contributes to Ethanol-Induced Liver Injury in Mice Linking Hepatocellular Death to Inflammation. Alcohol Clin Exp Res 41(4):719-26.
26. Hosoi T, Yokoyama S, Matsuo S, Akira S, Ozawa K (2010) Myeloid differentiation factor 88 (MyD88)-deficiency increases risk of diabetes in mice. PLoS One 5(9):e12537.

27. Garcia AD, Doan NB, Imura T, Bush TG, Sofroniew MV (2004) GFAP-expressing progenitors are the principal source of constitutive neurogenesis in adult mouse forebrain. Nat Neurosci 7(11):1233-41.
28. Grcevic D, Pejda S, Matthews BG, Repic D, Wang L, Li H, et al. (2012) In vivo fate mapping identifies mesenchymal progenitor cells. Stem Cells 30(2):187-96.
29. Vlantis K, Polykratis A, Welz PS, van Loo G, Pasparakis M, Wullaert A (2016) TLR-independent anti-inflammatory function of intestinal epithelial TRAF6 signalling prevents DSS-induced colitis in mice. Gut 65(6):935-43.
30. Yuan Q, Gu J, Zhang J, Liu S, Wang Q, Tian T, et al. (2021) MyD88 in myofibroblasts enhances colitis-associated tumorigenesis via promoting macrophage M2 polarization. Cell Rep 34(5):108724.
31. McCullough RL, McMullen MR, Das D, Roychowdhury S, Strainic MG, Medof ME, et al. (2016) Differential contribution of complement receptor C5aR in myeloid and non-myeloid cells in chronic ethanol-induced liver injury in mice. Mol Immunol 75:122-32.
32. Orlicky DJ, Roede JR, Bales E, Greenwood C, Greenberg A, Petersen D, et al. (2011) Chronic ethanol consumption in mice alters hepatocyte lipid droplet properties. Alcohol Clin Exp Res 35(6):1020-33.
33. Weiskirchen S, Tag CG, Sauer-Lehnen S, Tacke F, Weiskirchen R (2017) Isolation and Culture of Primary Murine Hepatic Stellate Cells. Methods Mol Biol 1627:165-91.
34. Hou S, Jiao Y, Yuan Q, Zhai J, Tian T, Sun K, et al. (2018) S100A4 protects mice from high-fat diet-induced obesity and inflammation. Lab Invest 98(8):1025-38.
35. Xiayu Rao XH, Zhicheng Zhou, Xin Lin (2013) An improvement of the 2^(-delta delta CT) method for quantitative real-time polymerase chain reaction data analysis. Biostat Bioinforma Biomath 3(3):71-85.
36. Yuan Q, Hou S, Zhai J, Tian T, Wu Y, Wu Z, et al. (2019) S100A4 promotes inflammation but suppresses lipid accumulation via the STAT3 pathway in chronic ethanol-induced fatty liver. J Mol Med (Berl) 97(10):1399-412.
37. Kiefer FW, Neschen S, Pfau B, Legerer B, Neuhofer A, Kahle M, et al. (2011) Osteopontin deficiency protects against obesity-induced hepatic steatosis and attenuates glucose production in mice. Diabetologia 54(8):2132-42.
38. Mohs A, Kuttkat N, Otto T, Youssef SA, De Bruin A, Trautwein C (2020) MyD88-dependent signaling in non-parenchymal cells promotes liver carcinogenesis. Carcinogenesis 41(2):171-81.
39. Roh YS, Seki E (2013) Toll-like receptors in alcoholic liver disease, non-alcoholic steatohepatitis and carcinogenesis. J Gastroenterol Hepatol 28 Suppl 1:38-42.
40. Yiu JH, Dorweiler B, Woo CW (2017) Interaction between gut microbiota and toll-like receptor: from immunity to metabolism. J Mol Med (Berl) 95(1):13-20.
41. Morales-Ibanez O, Dominguez M, Ki SH, Marcos M, Chaves JF, Nguyen-Khac E, et al. (2013) Human and experimental evidence supporting a role for osteopontin in alcoholic hepatitis. Hepatology 58(5):1742-56.

42. Icer MA, Gezmen-Karadag M (2018) The multiple functions and mechanisms of osteopontin. Clin Biochem 59:17-24.
43. Bruha R, Vitek L, Smid V (2020) Osteopontin - A potential biomarker of advanced liver disease. Ann Hepatol 19(4):344-52.
44. Seth D, Duly A, Kuo PC, McCaughan GW, Haber PS (2014) Osteopontin is an important mediator of alcoholic liver disease via hepatic stellate cell activation. World J Gastroenterol 20(36):13088-104.
45. Lancha A, Rodriguez A, Catalan V, Becerril S, Sainz N, Ramirez B, et al. (2014) Osteopontin deletion prevents the development of obesity and hepatic steatosis via impaired adipose tissue matrix remodeling and reduced inflammation and fibrosis in adipose tissue and liver in mice. PLoS One 9(5):e98398.
46. Ge X, Leung TM, Arriazu E, Lu Y, Urtasun R, Christensen B, et al. (2014) Osteopontin binding to lipopolysaccharide lowers tumor necrosis factor-alpha and prevents early alcohol-induced liver injury in mice. Hepatology 59(4):1600-16.
47. Arab JP, Roblero JP, Altamirano J, Bessone F, Chaves Araujo R, Higuera-De la Tijera F, et al. (2019) Alcohol-related liver disease: Clinical practice guidelines by the Latin American Association for the Study of the Liver (ALEH). Ann Hepatol 18(3):518-35.
48. Singh S, Osna NA, Kharbanda KK (2017) Treatment options for alcoholic and non-alcoholic fatty liver disease: A review. World J Gastroenterol 23(36):6549-70.
49. Anthoney N, Foldi I, Hidalgo A (2018) Toll and Toll-like receptor signalling in development. Development 145(9).
50. Diehl KL, Vorac J, Hofmann K, Meiser P, Unterweger I, Kuerschner L, et al. (2020) Kupffer Cells Sense Free Fatty Acids and Regulate Hepatic Lipid Metabolism in High-Fat Diet and Inflammation. Cells 9(10):2258.

Figures

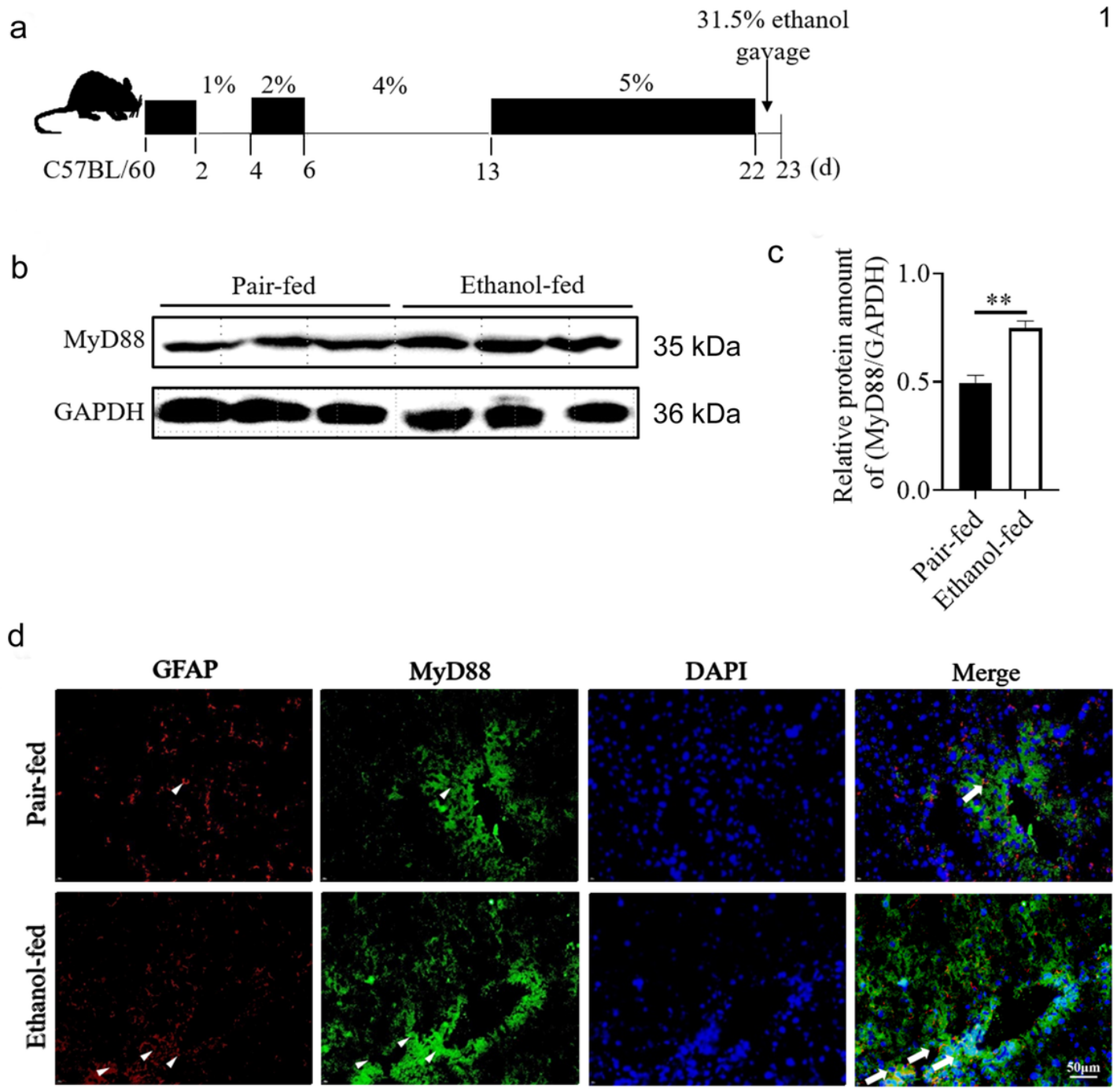

Figure 1

Expression of MyD88 is increased in the livers of ethanol-fed mice Groups of C57BL/6 mice (n=5 per group) were used to establish the chronic-binge ethanol model or fed an ethanol-free control liquid diet. a Schematic representation of the experimental procedure for the chronic-binge model. b, c MyD88 expression in livers were analyzed by Western blot and gray value. **p0.01. d Immunofluorescence staining of MyD88 and GFAP in liver tissues. Nuclei were counter-stained with DAPI. The arrows indicated GFAP+, MyD88+ and GFAP+MyD88+ cells, respectively. Scale bar=50 μm.

Figure 2

MyD88 deficiency in HSCs attenuates ethanol-induced liver injury Groups of MyD88fl/fl, MyD88GFAP-KO and MyD88SMA-KO mice (n=5 per group) were used to establish the chronic-binge ethanol model or fed an ethanol-free control liquid diet. a, b Changes in body weight of MyD88fl/fl, MyD88GFAP-KO and MyD88SMA-KO mice. c, d Changes in the liver/body weight of MyD88fl/fl, MyD88GFAP-KO and MyD88SMA-KO mice. *p□0.05. e-h The levels of serum ALT and AST in mice from different groups. *p□ 0.05. i, j Representative hematoxylin and eosin (H&E) staining of liver tissues in mice from different groups. Scale bar=100 μm.

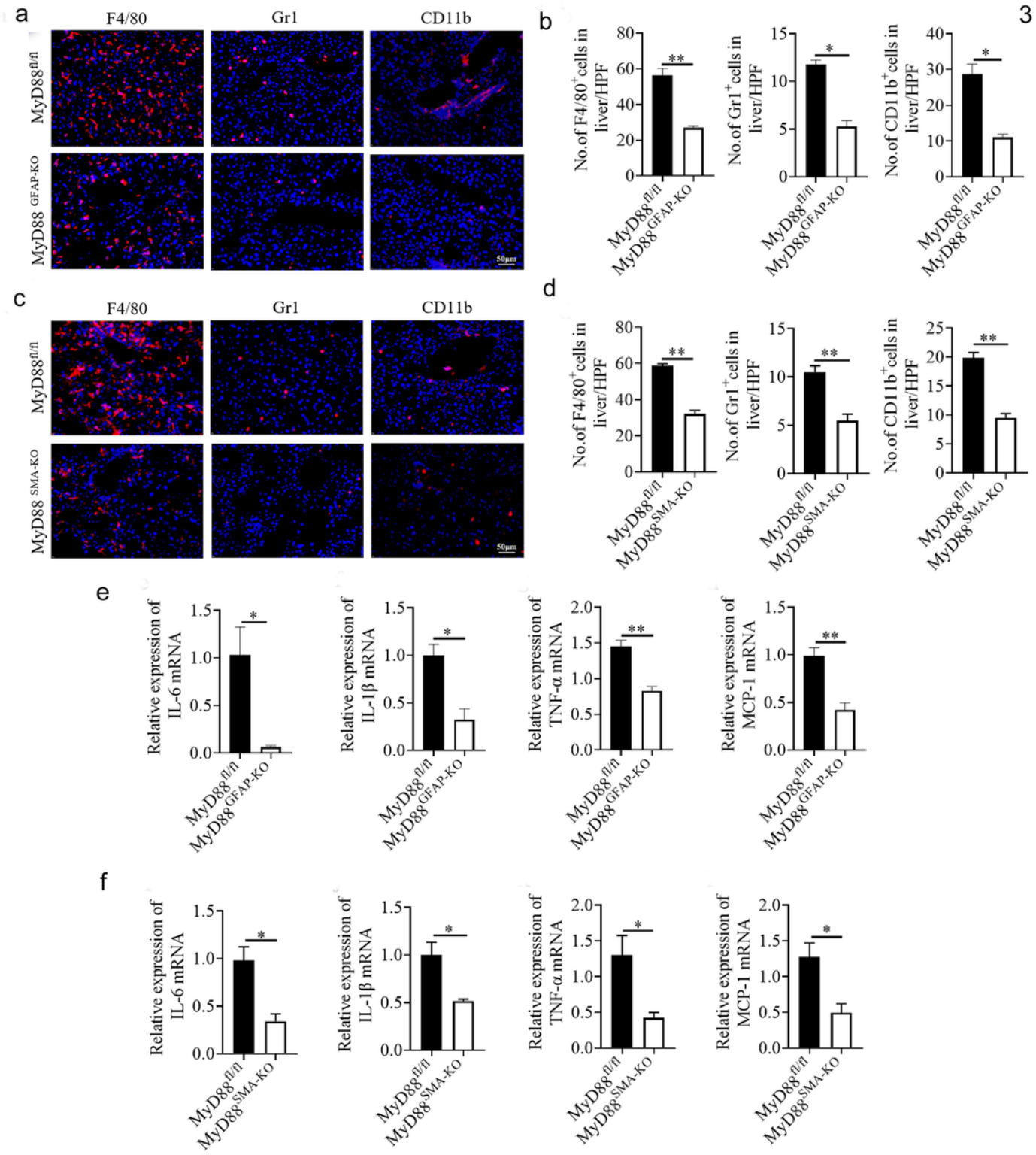

Figure 3

MyD88 deficiency in HSCs attenuates ethanol-induced liver inflammation Groups of MyD88fl/fl, MyD88GFAP-KO and MyD88SMA-KO mice (n=5 per group) were used to establish the chronic-binge ethanol model. a, c Immunofluorescence detection of F4/80+, Gr-1+ and CD11b+ cells infiltration in liver tissues of MyD88fl/fl, MyD88GFAP-KO and MyD88SMA-KO mice respectively. b, d Representative and statistical analysis of immunofluorescence staining for F4/80+, Gr-1+ and CD11b+ infiltration in liver

tissues of MyD88fl/fl, MyD88GFAP-KO and MyD88SMA-KO mice. HPF: High power field. *p0.05**p0.01. Scale bar=50 μm. e The mRNA levels of IL-6, IL-1β, TNF-α and MCP-1 in the liver tissues of MyD88fl/fl and MyD88GFAP-KO mice were measured using real-time PCR analysis. *p0.05**p0.01. f The mRNA levels of IL-6, IL-1β, TNF-α and MCP-1 in the liver tissue of MyD88fl/fl and MyD88SMA-KO mice were measured using real-time PCR analysis. *p0.05.

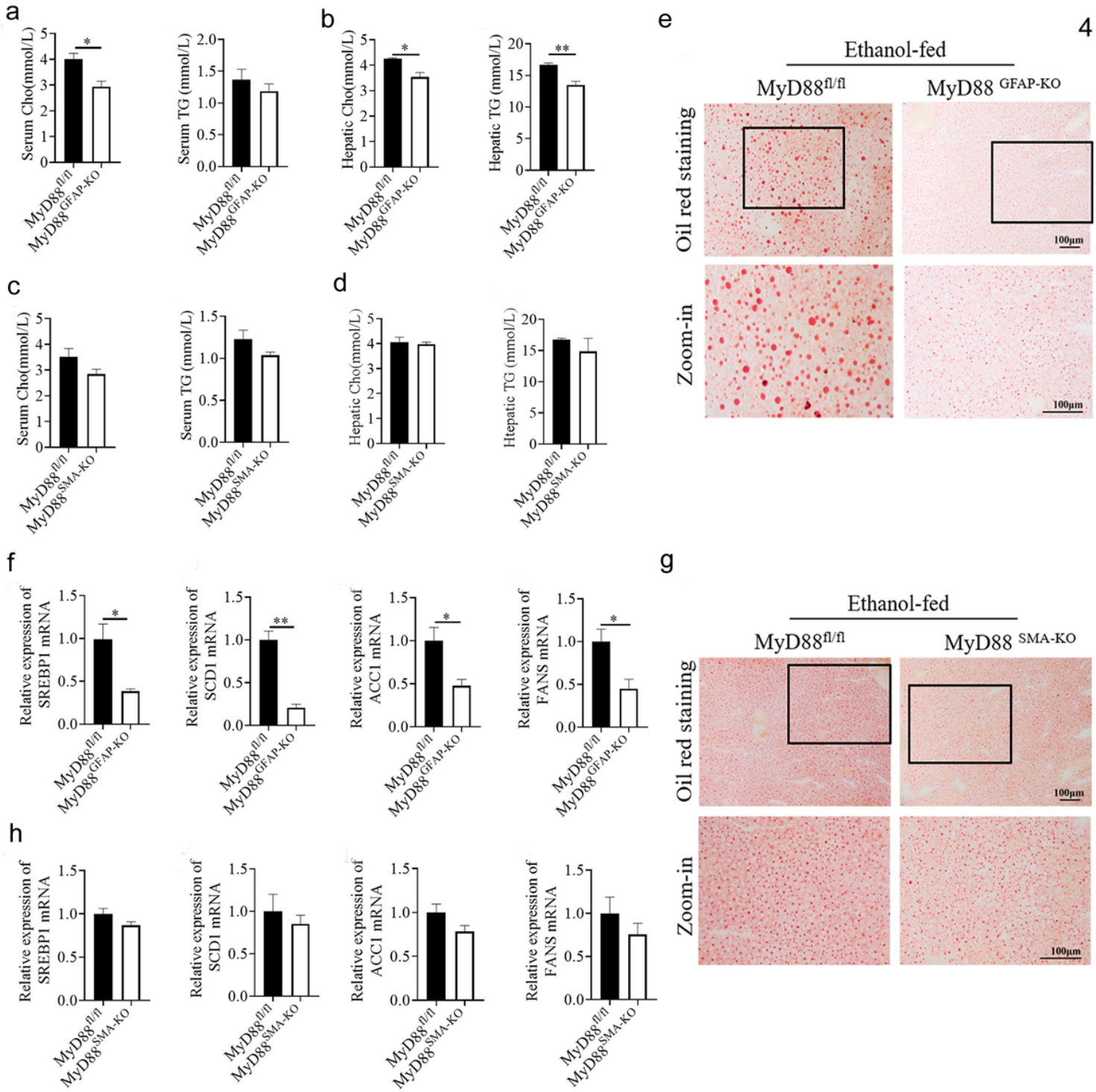

Figure 4

MyD88 deficiency in quiescent HSCs attenuates liver fat accumulation Groups of MyD88fl/fl, MyD88GFAP-KO and MyD88SMA-KO mice (n=5 per group) were used to establish the chronic-binge ethanol model. a Serum cholesterol (Cho) and triglyceride (TG) levels of MyD88fl/fl and MyD88GFAP-KO mice. b Hepatic Cho and TG levels of MyD88fl/fl and MyD88GFAP-KO mice. *p□0.05. **p□0.01. c Serum Cho and TG levels of MyD88fl/fl and MyD88SMA-KO mice. d Hepatic Cho and TG levels of MyD88fl/fl and MyD88SMA-KO mice. e, g Oil red O staining of liver tissues of MyD88fl/fl, MyD88GFAP-KO and MyD88SMA-KO mice. Scale bar=100 μm. f, h The mRNA levels of SREBP1□SCD1□ACC1 and FANS in livers of MyD88fl/fl, MyD88GFAP-KO and MyD88SMA-KO mice were measured using real-time PCR analysis. *p□0.05□**p□0.01.

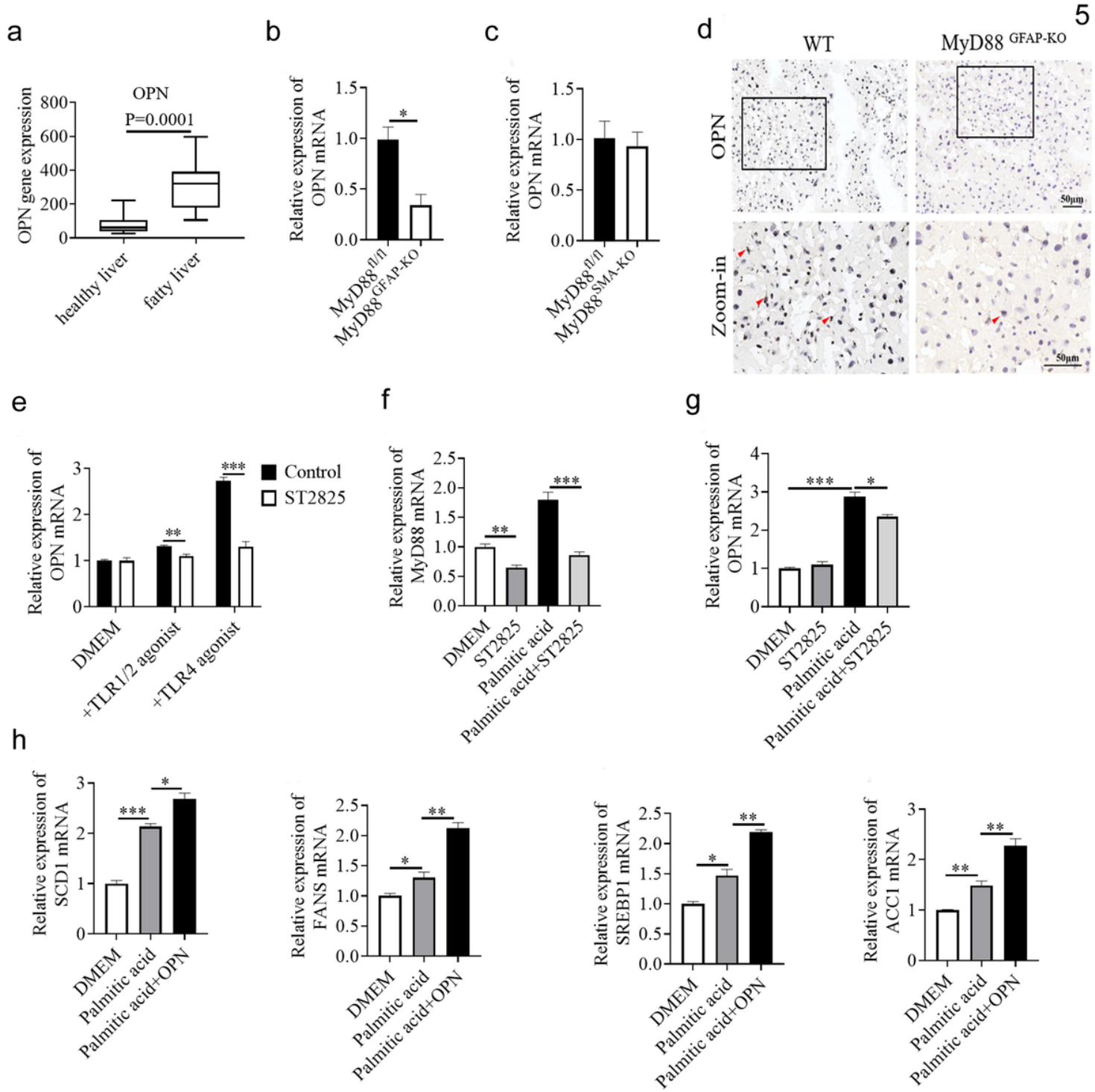

Figure 5

MyD88 deficiency in HSCs downregulated OPN expression a GEO database analyzed the expression level of OPN in the liver of healthy and fatty liver patients. b, c Groups of MyD88fl/fl, MyD88GFAP-KO and MyD88SMA-KO mice (n = 5 per group) were used to establish the chronic-binge ethanol model. The mRNA levels of OPN in the livers of MyD88fl/fl, MyD88GFAP-KO and MyD88SMA-KO mice were measured using real-time PCR. *p<0.05. d Immunohistochemical detection of OPN in liver tissues of MyD88fl/fl and MyD88GFAP-KO mice. Scale bar=50μm. e LX-2 cells were treated with MyD88 inhibitor

ST2825 for 2h and then was treated with TLR1/2 and TLR4 agonists for 24h. The mRNA levels of OPN were measured using real-time PCR. **p□0.01. f, g LX-2 cells were exposed to ST2825 (20 μM) (MedChemExpress, USA) for 2 h, and then were challenged with TLR1/2 agonist (Pam3CSK4, 100 ng/mL), TLR4 agonist (LPS, 1 mg/mL) and palmitic acid (400 μM) respectively for 24 h. In the control groups, LX-2 cells were directly challenged with TLR1/2 agonist (Pam3CSK4, 100 ng/mL), TLR4 agonist (LPS, 1 mg/mL) and palmitic acid (400 μM) respectively for 24 h. The mRNA level of MyD88 and OPN in LX-2 cells were measured using real-time PCR. **p□0.01. h HepG2 cells were exposed to DMEM medium with 400 μM palmitic acid for 24 h and then 200 ng/mL recombinant protein OPN for 24h. The SCD1, FANS, SREBP1 and ACC1 mRNA expression levels in HepG2 cells were measured using real-time PCR. *p□ 0.05, **p□0.01.

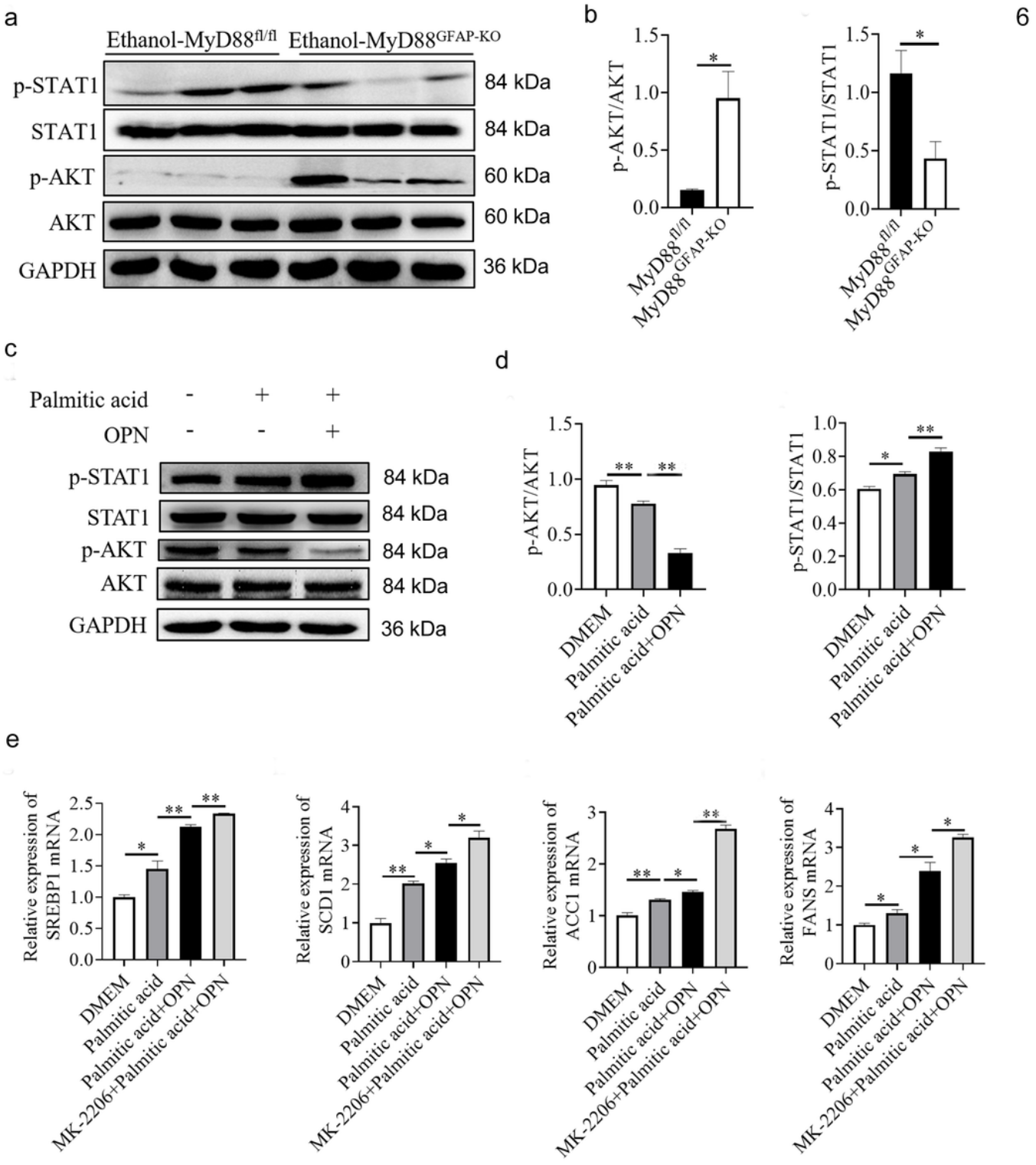

Figure 6

MyD88 in HSCs promoted liver fat accumulation and inflammation via the AKT pathway and STAT1 pathway respectively Groups of MyD88fl/fl, MyD88GFAP-KO and MyD88SMA-KO mice (n=5 per group) were used to establish the chronic-binge ethanol model. a, b The protein levels of AKT, p-AKT, STAT1and p-STAT1 in livers were determined by Western blot. The densities of proteins were quantified using densitometry. Phospho-proteins were normalized to total proteins. *p<0.05. c, d HepG2 cells were treated

with 400 μM palmitic acid for 24h and then 200 ng/mL recombinant protein OPN for 24h. The protein levels of AKT, p-AKT, STAT1 and p-STAT1 in HepG2 cells were determined by Western blot. Phospho-proteins were normalized to total proteins. **p<0.01. e HepG2 cells were treated with OPN and the AKT inhibitor MK-2206 for 24 h. The mRNA levels of SREBP1、SCD1、ACC1 and FANS in HepG2 cells were measured using real-time PCR analysis. The results were normalized to GAPDH. *p<0.05, **p<0.01.

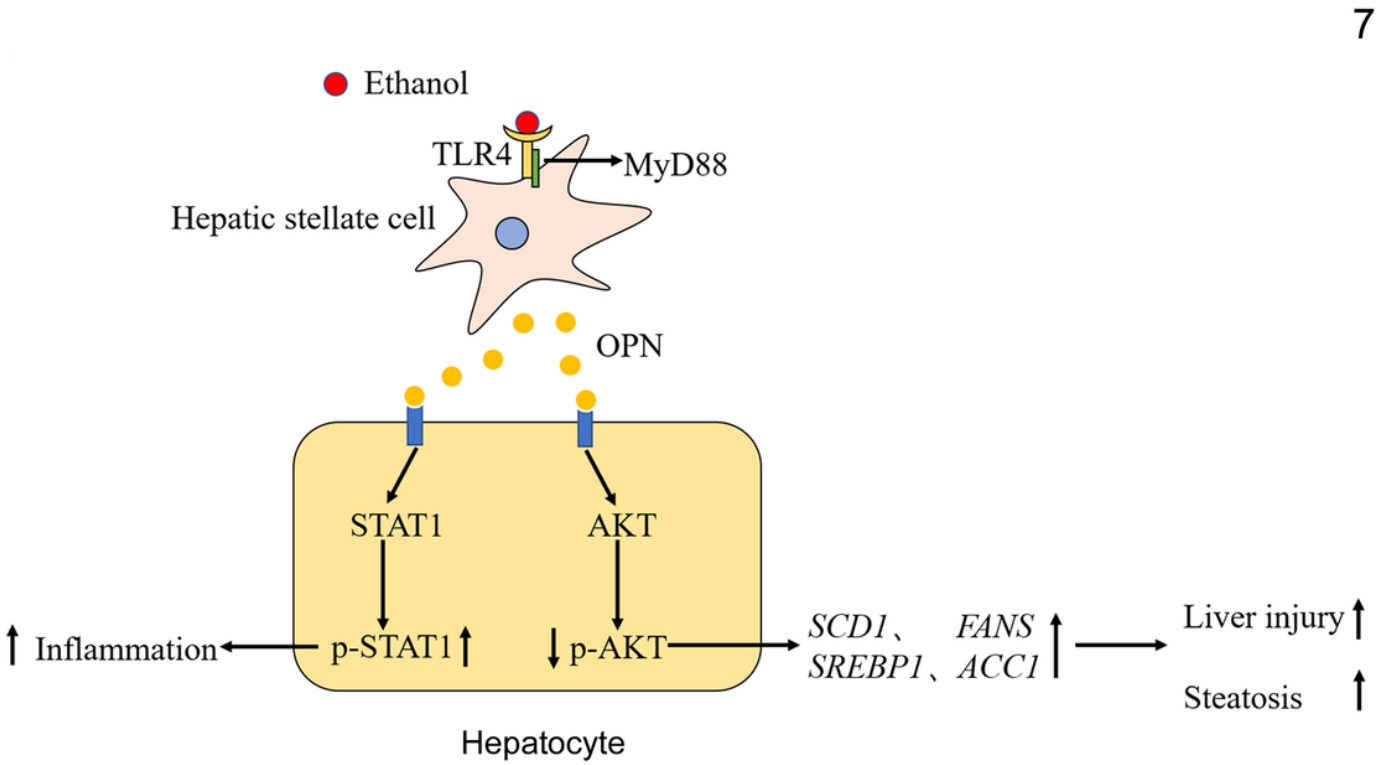

Figure 7

Schematic diagram of the promotion mechanism of MyD88 in quiescent HSCs on HepG2 cells adipogenesis and inflammation Ethanol activated the MyD88-dependent TLR4 signaling pathway in quiescent HSCs, thereby promoting the secretion of OPN in quiescent HSCs. The secreted OPN acted on AKT in HepG2 cells, inhibited the phosphorylation of AKT and further promoted adipogenesis and liver injury. In addition, the secreted OPN also promoted the phosphorylation of STAT1 in HepG2 cells and played a role in promoting inflammation.

Supplementary Files

This is a list of supplementary files associated with this preprint. Click to download.

- Supplementalmaterial.docx